



Nanoparticle Growth by Particle Phase Chemistry

Michael J. Apsokardu and Murray V. Johnston

Department of Chemistry and Biochemistry, University of Delaware, Newark, DE, 19716, USA

Correspondence to: Murray V. Johnston (mvj@udel.edu)

5 Abstract

The ability of particle phase chemistry to alter the molecular composition and enhance the growth rate of nanoparticles in the 2-100 nm diameter range is investigated through the use of a growth model. The molecular components included are sulfuric acid, ammonia, water, a non-volatile organic compound and a semi-volatile organic compound. Molecular composition and growth rate are compared for particles that grow by partitioning alone vs. those that grow by a combination of partitioning and an accretion reaction in the particle phase between two organic molecules. Particle phase chemistry causes a change in molecular composition that is particle diameter dependent, and when the reaction involves semi-volatile molecules, the particles grow faster than by partitioning alone. These effects are most pronounced for particle larger than about 20 nm in diameter. The growth rate enhancement increases linearly with increasing particle diameter and is dependent on the gas phase mixing ratio of the semi-volatile reactant and the reaction rate constant. The results are discussed in the context of recent experimental measurements of particle size-dependent molecular composition and the relationship between accretion product formation and cloud condensation nuclei (CCN) activity.

1 Introduction

Atmospheric aerosols influence Earth's energy balance either directly by scattering incoming solar radiation or indirectly through cloud formation (Charlson et al., 1992; Kerminen et al., 2012; Lohmann and Feichter, 2004). A significant fraction of airborne particles originate from gas-to-particle conversion during new particle formation (NPF) (Bzdek and Johnston, 2010). Volatile compounds emitted into the atmosphere from biogenic and anthropogenic sources are oxidized to produce semi-volatile and non-volatile products. Particle formation begins when these products in combination with other gas phase species come together to form clusters on the order of 1-2 nm in diameter that are able to spontaneously grow to much larger sizes (Bzdek and Johnston, 2010; Dusek et al., 2006; Kulmala et al., 2013; Zhang et al., 2012). Depending on chemical composition, once the particles have grown to a size of 50-100 nm in diameter, they are able to serve as cloud condensation nuclei (CCN). The probability that a newly formed nanoparticle will grow to a CCN relevant size depends on its growth rate relative to the loss rate from e.g. coagulation or scavenging by pre-existing aerosols (Kuang et al., 2010). Uncertainties in predicting the conditions that favor in CCN formation make it challenging to accurately predict future impacts of radiative forcing (Carslaw et al., 2013).



The three main chemical species that contribute to ambient nanoparticle growth are sulfuric acid, a neutralizing base typically ammonia, and organic matter. The growth rate due to sulfuric acid along with
35 neutralizing base is accurately predicted by a condensational growth model (Bzdek et al., 2011, 2012, 2013;
Pennington et al., 2013), though sulfuric acid represents only a minor fraction of the total growth rate of ambient
particles (Kuang et al., 2010, 2012; Weber et al., 1996). Nanoparticle composition and growth rate are dominated by
organic matter (Bzdek et al., 2011, 2012, 2013, 2014a, 2014b; Pennington et al., 2013; Riipinen et al., 2012), but
current growth models for organic matter appear to be incomplete (Bianchi et al., 2016; Ehn et al., 2014; Jimenez et
40 al., 2009; Kulmala et al., 2013; Riccobono et al., 2014; Tröstl et al., 2016).

Gas phase oxidation of volatile organic compounds occurs through a complex set of reaction pathways
yielding many gas and particle phase products, often numbering in the hundreds or thousands based on accurate
mass measurements (Bateman et al., 2008; Heaton et al., 2009; Reinhardt et al., 2007; Tu et al., 2016). Absorptive
partitioning (Barsanti et al., 2017; Pankow, 1994) of gas phase products to the particle phase forms secondary
45 organic aerosol (SOA), which includes both non-volatile (NVOC) and semi-volatile (SVOC) organic compounds
(Kroll and Seinfeld, 2008; Riipinen et al., 2012). NVOC have a negligible evaporation rate after partitioning to the
particle phase, and therefore cause particles to grow at a rate given by the condensation rate. SVOC have a
significant evaporation rate from the particle phase, and therefore grow particles at a slower rate than the
condensation rate. Recent advances in measurement technology have greatly improved our molecular understanding
50 of NVOC (Ehn et al., 2012, 2014; Jokinen et al., 2015). More broadly, the complex distribution of molecular
products and their associated wide range of volatilities can be represented by a volatility basis set (VBS) distribution
where products are binned according to their gas phase saturation concentrations (Donahue et al., 2006, 2011a,
2012). VBS distributions are an effective means of modeling SOA growth on the basis of molecular partitioning
(Donahue et al., 2011b; Tröstl et al., 2016; Trump and Donahue, 2014).

Molecular analysis of SOA has shown the presence of compounds that were produced by a reaction within
the particle phase. Some examples include oligomers in biogenic SOA formed by accretion reactions (Barsanti and
Pankow, 2004; Kalberer et al., 2004; Tolocka et al., 2004a), imine related species formed by the reaction of
dicarbonyls with ammonia or amines (DeHaan et al., 2011; Galloway et al., 2014; Lee et al., 2013; Stangl and
Johnston, 2017), and organosulfates (Riva et al., 2016; Surratt et al., 2007; Wong et al., 2015; Xu et al., 2015).
60 Reactions such as these increase the aerosol yield by forming additional SOA beyond what would be expected from
partitioning alone if they form non-volatile products from semi-volatile reactants in the particle phase (Lopez-
Hilfiker et al., 2016; Shiraiwa et al., 2014). Recent measurements of accretion reaction products have shown that
their particle phase concentrations increase with increasing particle size as would be expected for a process limited
by available particle volume (Shiraiwa et al., 2013; Tu and Johnston, 2017; Wu and Johnston, 2017).

Since particle phase chemistry is able to increase the aerosol yield, it is reasonable to expect that particle
phase chemistry may also increase the nanoparticle growth rate. In this work, we explore the possibility of a growth
rate enhancement using a simplified model relevant to NPF. In the first set of calculations, chemical composition
and growth rate are determined for particles between 2 and 100 nm assuming that growth occurs by partitioning



70 alone. These results are compared to a second set of calculations where semi-volatile molecules in the particle phase are allowed to undergo an accretion reaction to produce a non-volatile product. Together, the two sets of calculations give insight into the experimental conditions and particle size range where particle phase chemistry is most likely to alter nanoparticle composition and accelerate the growth rate.

2 Model Description

75 The growth model used in this work includes sulfuric acid, ammonia, and SOA since these are the major components found in ambient nanoparticles during NPF (Bzdek et al., 2011, 2012, 2013, 2014a; Pennington et al., 2013). Water is also included as predicted by the Extended Aerosol Inorganics Model (E-AIM) (Wexler and Clegg, 2002), and then corrected to account for the effects of particle surface curvature (Kreidenweis et al., 2005; Yli-Juuti et al., 2013). For simplicity, the gas phase precursors to SOA formation are represented by two specific compounds,
80 one non-volatile (NVOC) and the other semi-volatile (SVOC). Particle phase chemistry involves a simple accretion reaction between two SVOC (or NVOC) molecules to give a dimer. Table 1 gives relevant molecular parameters and gas phase mixing ratios. For the calculations performed here, gas phase mixing ratios are assumed to be constant over time, and the values chosen are typical of what might be observed during NPF in a boreal forest (Vestenius et al., 2014). Molecular volatility is expressed in terms of the saturation concentration, C^* , which is the
85 equilibrium vapor pressure in units of $\mu\text{g}/\text{m}^3$ (Donahue et al., 2006).

Calculations begin with a 2 nm diameter particle consisting of sulfuric acid and ammonia in a 2:1 ratio of base to acid. From there, gas phase species partition to the particle phase based on their volatilities and gas phase mixing ratios, causing the particle to grow. The growth calculation is iterative. Starting from an initial particle of a given composition and volume ($V_{p,n}$), the increase in particle volume (and corresponding change in composition) is
90 determined over a short time period for each molecular species separately, and the increases for the individual components are summed to give the total volume of the particle at the end of the time period ($V_{p,n+1}$) along with its composition. The end point for the first time period is used as the start point for the second time period, and the process repeats. A schematic of calculation of work flow is given in Supporting Information Figure S1 along with additional aspects of the approach.

95 2.1 Partitioning

The extent to which a compound formed in the gas phase partitions to the particle phase is determined by its saturation ratio (S_D), which is the ratio of the gas phase mixing ratio to the saturation mixing ratio. The subscript “D” acknowledges that the saturation ratio depends in part on the radius of curvature of the particle surface. Accordingly, the first step in the calculation is to determine the Kelvin effect modified vapor pressure ($KEMP_D$) for
100 all species based on the initial particle diameter. For the conditions used in this study, sulfuric acid and NVOC have $S_D \gg 1$ for all particle diameters investigated, and as discussed previously, grow particles at their condensation rates. Ammonia, water, and SVOC have $S_D \ll 1$ and grow particles at rates slower than their condensation rates.



The collision rate for species i determines the number of condensing molecules that can be taken into the particle during time period dt , thereby incrementing the particle volume by dV_i :

$$(1) \quad \frac{dV_i}{dt} = \frac{c_i}{4} \gamma \pi D^2 C_{i,g} \beta_D V_{M,i}$$

where c_i is the mean thermal velocity, γ is the uptake coefficient, D is the particle diameter, $C_{i,g}$ is the gas phase mixing ratio of species i , β_D is the Fuchs-Sutugin correction factor for mass transport to a spherical particle with diameter D , and $V_{M,i}$ is the molar volume of species i . The equation for β_D is given in Supporting Information. Values of dV_i for condensational growth by sulfuric acid and NVOC are calculated from Eq. 1, with the inherent assumptions that the surface accommodation coefficient is 1, and the particle diameter is small enough that gas phase diffusion does not limit the condensation rate.

Equation 1 can also be used to calculate the uptake of semi-volatile species provided that the total amount taken into the particle does not exceed the equilibrium end point. Ammonia uptake is determined from the number of sulfuric acid molecules that have condensed. For a given time period dt , once the number of ammonia molecules that have been taken into the particle equals twice the number of sulfuric acid molecules that were taken during the same time period, no further ammonia uptake occurs. While dissolution of ammonia into water is possible, the amount is negligible in comparison to ammonia uptake associated with condensation of sulfuric acid (Clegg et al., 1998; Wexler and Clegg, 2002). Under the conditions used in this study, the condensation rate of ammonia is about 25 times greater than that of sulfuric acid, so the model assumes that stoichiometric uptake of ammonia is essentially instantaneous with sulfuric acid. Water uptake is determined from E-AIM based on the combined amounts of sulfuric acid, ammonia, and NVOC that have been added during time period dt . Since the gas phase mixing ratio of water is very high, equilibrium is assumed to be achieved instantaneously during the time period.

Individual volume increments dV_i for sulfuric acid, NVOC, ammonia, and water are summed to give the total volume increment. Because the volume of particle phase has increased, SVOC is no longer in equilibrium between the gas and particle phases, and a net migration of SVOC from the gas phase to the particle phase must occur. SVOC molecules are taken into the particle at a rate described by Eq. 1 to re-establish equilibrium. The equilibrium point (Pankow, 1994) expressed as the volume ratio of SVOC in the particle phase ($V_i/V_{p,n}$) is:

$$(2) \quad \frac{V_i}{V_{p,n}} = \left(\frac{C_{i,g}}{KEMP_D} \right) \left(\frac{V_{M,i}}{V_{M,p}} \right) \frac{1}{\zeta_i}$$

where i in this case refers to SVOC, ζ_i is the activity coefficient for SVOC in the particle phase (assumed to be 1 in this study), and $V_{M,i}$ and $V_{M,p}$ are the respective the molar volumes of SVOC and the particle phase. The incremental increase of SVOC over time period dt is determined by evaluating Eq. 2 before and after the increases due to sulfuric acid, NVOC, ammonia, and water. For the conditions used in this study, the condensation rate of gas phase SVOC is uniformly greater than the uptake rate needed to maintain equilibrium when particle growth is restricted to partitioning. The ratio of the two rates is dependent on the volume to surface area ratio of the particle, ranging from several orders of magnitude for a 2 nm diameter particle to a factor of 200 for a 100 nm diameter particle. Because the condensation rate is generally much greater than the uptake rate needed for partitioning, no evaporation rate of



particle phase SVOC was included in the current study. The one situation where condensation is not sufficient for partitioning occurs when particle phase chemistry is considered and will be discussed later.

2.2 Particle Phase Chemistry

140 Particle phase chemistry is modeled as an irreversible accretion reaction where two SVOC molecules come
together to form a non-volatile DIMER:

$$(3) \quad \frac{d[DIMER]}{dt} = - \frac{d[SVOC]}{dt} = k_{DIMER}[SVOC]^2$$

where k_{DIMER} is the second order rate constant and $[SVOC]$ is the particle phase concentration established by
partitioning between the gas and particle phases. Since the reaction consumes particle phase SVOC molecules,
145 additional SVOC must be taken from the gas phase into the particle phase to re-establish equilibrium. The rate at
which additional SVOC molecules are taken into the particle is determined by the rate of particle phase reaction.
When particle phase reaction is included in the growth calculation, the change in particle volume from $V_{p,n}$ to $V_{p,n+1}$
with respect to SVOC is the sum of the volume increase from unreacted SVOC molecules needed to re-establish
partitioning equilibrium and the volume increase from additional SVOC uptake to form dimers. SVOC continues to
150 partition to the particle phase at each iteration, resulting in a continuous supply of reactant molecules for
dimerization. Most calculations were performed with a dimerization rate constant of $10^{-2} \text{ M}^{-1} \text{ s}^{-1}$, which is the rate
constant reported for dimerization of glyoxal in a bulk aqueous solution (Ervens and Volkamer, 2010). The effects
of particle phase diffusion coefficient and phase separation are not considered in this work, though we note that both
would have the effect of reducing the impact of particle phase chemistry on composition and growth rate.

155

3 Results and Discussion

3.1 Particle Growth by Partitioning

The first set of calculations includes particle growth by partitioning, but no particle phase reaction. Figure
1a shows the diameter growth rate and Figure 1b the dry mass fraction for each chemical species as a function of
160 particle diameter. Initially, the diameter growth rates for all species increase quickly with increasing particle size.
For sulfuric acid and NVO, the increase is most pronounced between 2 and 10 nm, and this size dependence arises
directly from the Fuchs-Sutugin term that limits mass transport to small diameter particles. Above about 10 nm, the
growth rates for these species become independent of particle diameter. A constant growth rate for non-volatile
species has been noted previously (Weber et al., 1996) and can be understood by rewriting Eq. 1 in terms of the
165 diameter growth rate:

$$(4) \quad \frac{dD}{dt} = \frac{c_i}{2} \gamma C_{i,g} \beta_D V_{M,i}$$

Above about 10 nm, β_D becomes independent of D . Since γ is independent of D for a surface-limited process such
as condensation (Smith et al., 2003; Tolocka et al., 2004a), dD/dt also becomes independent of D provided that the



precursor gas phase mixing ratio ($C_{i,g}$) does not change. Ammonia uptake is driven by sulfuric acid uptake, and
170 therefore follows the same particle diameter dependence.

Water and SVOC show greater increases in their growth rates with increasing particle diameter than sulfuric acid and NVOC because they have $S_D < 1$. In principle, semi-volatile species are subject to two particle size-dependent effects: β_D in Eq. 1 and $KEMP_D$ in Eq. 2. For the conditions studied here, the β_D term has a negligible effect on the uptake rates of water and SVOC, since uptake is determined by the equilibrium endpoint
175 rather than the condensation rate. Instead, the difference between the semi-volatile species and non-volatile species in Figure 1a are driven by the particle size dependence of $KEMP_D$, which alters the equilibrium point for absorptive partitioning.

In Figure 1b, the dry particle mass fractions of sulfuric acid, NVOC, and ammonia show very little change with increasing D since their relative growth rates are independent of D . Small changes just above 2 nm are due to
180 the choice of starting composition of the 2 nm diameter particle. In contrast, the SVOC mass fraction increases quickly with increasing particle size owing to the dependence of $KEMP_D$ on D . Figure 2 shows the mass fraction ratio of SVOC to NVOC as a function of particle size. The ratio increases quickly at the smallest particle sizes and then more slowly thereafter. This plot is consistent with experimental measurements of molecular composition across a similar range of particle diameters, which show that lower volatility species are preferentially detected in
185 smaller particles (Winkler et al., 2012; Zhao et al., 2013).

3.2 Particle Growth by a Combination of Partitioning and Particle Phase Chemistry

When particle phase reaction is included in the growth calculation, both the growth rate and chemical composition change. Figures 3a and b show diameter growth rates and dry mass fractions, respectively, when particle phase reaction is included. Comparing Figure 3a to 1a shows that particle phase chemistry causes the
190 diameter growth rate to continue increasing with increasing particle size above 10 nm. This diameter dependence is different from the growth rate due to partitioning alone where dD/dt becomes independent of particle size above 10 nm. The size dependence of particle growth at larger particle sizes can be understood by expressing the uptake coefficient in terms of particle diameter:

$$(5) \quad \gamma = k'D .$$

In Eq. 5, the uptake coefficient is proportional to D , which is characteristic of a volume-limited process (Saul et al., 2006; Tolocka et al., 2004b). Inserting Eq. 5 into Eq. 4, shows that dD/dt also increases linearly with D . The number of SVOC molecules that react to form DIMER is proportional to the total volume of the particle, and therefore the SVOC uptake rate needed to maintain partitioning equilibrium is also volume (and hence diameter)
195 dependent. Note that the SVOC and DIMER diameter growth rates are both proportional to D in Figure 3a. Growth by condensation of NVOC and sulfuric acid remain surface-limited, and therefore, these diameter growth rates are
200 unaffected by dimer formation.



Figure 3b shows the dry mass fractions as a function of particle diameter when particle phase chemistry is included. Below about 10 nm, the plots in Figure 3b are identical to those in Figure 1b where partitioning alone is considered. Particle phase chemistry has minimal impact on the growth and composition of small particles for two reasons. First, the particle volume to surface area ratio is very small, which favors surface-limited processes (condensational growth by NVOC and sulfuric acid) over volume-limited processes (accretion reaction). Second, the dependence of $KEMP_D$ on D causes the equilibrium concentration of SVOC in the particle phase to be very low for small particles, which decreases the reaction rate (Eq. 3). As a result, particle phase chemistry has little impact on the diameter growth rate or molecular composition below about 10 nm. Above 10 nm, DIMER mass starts to accumulate in the particle, causing the mass fractions of NVOC, sulfuric acid, and ammonia decrease.

Figure 4a shows the mass fraction ratio of SVOC to NVOC as a function of particle diameter. Below 10 nm, where particle phase chemistry has minimal impact, the ratio in Figure 4a for particle phase reaction is equivalent to that in Figure 2 for partitioning alone. The plots in Figures 2 and 4a diverge above about 10 nm because the DIMER mass fraction increases, causing the NVOC mass fraction to decrease.

Figure 4b shows the mass fraction ratio of DIMER to NVOC. Below about 10 nm, hardly any DIMER is produced. Above 10 nm, the DIMER to NVOC ratio increases approximately linearly with increasing D as expected for a volume-limited process relative to a surface-limited process. Figures 3 and 4 show that particle size dependencies of the growth rate and composition above 10 nm are driven mainly by particle phase chemistry rather than partitioning alone. Figure 4b illustrates how the impact of an accretion reaction might be observed experimentally through organic molecular composition measurements. If a systematic increase in the concentration of non-volatile dimers and higher order oligomers is observed with increasing particle diameter, then accretion chemistry is likely to have contributed to the formation of these molecules. Accretion chemistry, however, is not necessarily limited to the reaction of SVOC. If NVOC in the particle phase reacts to form DIMER, then the diameter growth rate will *not* change with increasing particle diameter since NVOC uptake remains unaffected, though the molecular composition will change. A calculation demonstrating this principle is shown in Figures S2 and S3.

3.3 Factors that Influence Growth by Particle Phase Chemistry

Additional calculations were performed to investigate the roles of SVOC gas phase mixing ratio and particle phase reaction rate constant on growth rate and composition. In Figure 5a, diameter growth rates are shown for SVOC gas phase mixing ratios between 0.35 to 1.4 ppt and compared to the partitioning calculation in Figure 1a (the “1.4 ppt- NR” plot for no reaction in Figure 5a). Above about 10 nm, the growth rates increase linearly with increasing D , and the slope of the increase scales by approximately $[SVOC]^2$ as expected by Eq. 3. The actual dependence is slightly less than $[SVOC]^2$ owing to the change in particle density that is associated with the changing DIMER mass fraction.

Figure 5b shows the effect of reaction rate constant on diameter growth rate. The range of rate constants investigated ranges two orders of magnitude from 10^{-3} to $10^{-1} \text{ M}^{-1}\text{s}^{-1}$ while keeping the SVOC mixing ratio constant



at 1.4 ppt. “NR” in Figure 5b represents no reaction and is equivalent to the plot in Figure 1a for growth by partitioning alone. For a reaction rate constant of $10^{-3} \text{ M}^{-1}\text{s}^{-1}$, particle growth rate is only slightly larger than growth by partitioning only. In this case, DIMER production is slow, so there is little enhancement of the overall growth rate. Increasing the rate constant one order of magnitude to $10^{-2} \text{ M}^{-1}\text{s}^{-1}$, causes a substantial enhancement of the growth rate above 10 nm. For a rate constant of $10^{-1} \text{ M}^{-1}\text{s}^{-1}$, a complex plot is observed. Volume-limited particle growth occurs up to ~ 40 nm where the growth rate increases linearly with D . Above ~ 40 nm, the reaction rate becomes so fast that particle growth is limited by the condensation rate of SVOC, a surface-limited process, and the diameter growth rate and molecular composition become independent of D . Since the calculation methodology used in our study did not include an evaporation rate for SVOC, the transition from volume-limited to surface-limited kinetics is abrupt in Figure 5b. In practice, one would expect a more gradual transition from one to the other. The lack of a particle size dependence on SOA growth in the limit of a fast reaction rate has also been suggested in a modeling study of SOA produced by α -pinene ozonolysis (Gatzsche et al., 2017).

250 4 Atmospheric Implications

The work presented here shows that particle phase chemistry has the potential to both alter the composition and enhance the growth rate of sub-100 nm diameter particles. Recent experimental measurements of molecular composition have shown that accretion reaction product formation increases linearly with increasing aerosol volume to surface area (V/SA) ratio between about 7 and 35 nm – a similar V/SA range to the particle diameters considered here (Tu and Johnston, 2017; Wu and Johnston, 2017). The results presented here provide a fundamental basis for understanding molecular composition changes like these in the sub-100 nm diameter range.

While changes in molecular composition are well established experimentally, an enhancement of the particle growth rate in the sub-100 nm diameter range is less clear. Recent measurements by Kourtchev et al. (Kourtchev et al., 2016) of accretion oligomers in ambient aerosol from a boreal forest suggest that oligomer formation increases with increasing SOA mass concentration, an observation that is consistent with the molecular composition results reported here. More importantly, the authors noted that aerosols enriched with oligomers were strongly correlated with higher CCN activity, and they suggested that this correlation could indicate that oligomers may speed up particle growth. The results presented here show that particle phase reactions are indeed capable of enhancing growth rates in a size range relevant to CCN activity. Future experimental measurements should focus on growth rate measurements in the 10-100 nm diameter range and the physical parameters (reaction rate constant, particle phase diffusion constant, phase separation, etc.) (Liu et al., 2014; Mai et al., 2015; Riipinen et al., 2012; Shiraiwa et al., 2012; Song et al., 2015; Zaveri et al., 2014) that may influence the contribution of particle phase chemistry to the growth rates of these particles.

270 Supporting Information



Three figures (S1-S3) plus additional description of the particle growth model.

Acknowledgements

This research was supported by the National Science Foundation under grant number CHE-1408455.



References

- 275 Barsanti, K. C. and Pankow, J. F.: Thermodynamics of the formation of atmospheric organic particulate matter by accretion reactions-Part 1: aldehydes and ketones, *Atmos. Environ.*, 38, 4371–4382, doi:10.1016/j.atmosenv.2006.03.013, 2004.
- Barsanti, K. C., Kroll, J. H. and Thornton, J. A.: The Formation of Low-Volatility Organic Compounds in the Atmosphere: Recent Advancements and Insights, *J. Phys. Chem. Lett.*, DOI: 10.1021/acs.jpcclett.6b02969, doi:10.1021/acs.jpcclett.6b02969, 2017.
- 280 Bateman, A. P., Walser, M. L., Desyaterik, Y., Laskin, J., Laskin, A., Nizkorodov, S. A. and Bateman, A. P.: The Effect of Solvent on the Analysis of Secondary Organic Aerosol Using Electrospray Ionization Mass Spectrometry, *Environ. Sci. Technol.*, 42(19), 7341–7346, doi:10.1021/es801226w, 2008.
- Bianchi, F., Junninen, H., Frege, C., Henne, S., Hoyle, C. R., Molteni, U., Herrmann, E., Adamov, A., Bukowiecki, N., Chen, X., Duplissy, J., Gysel, M., Hutterli, M., Kangasluoma, J., Kontkanen, J., Manninen, H. E., Rondo, L., Williamson, C., Curtius, J., Worsnop, D. R., Kulmala, M., Dommen, J. and Baltensperger, U.: New particle formation in the free troposphere: A question of chemistry and timing, *Science*, 352(6289), 1109–1112, doi:10.1126/science.aad5456, 2016.
- 285 Bzdek, B. R. and Johnston, M. V.: New Particle Formation and Growth in the Troposphere, *Anal. Chem.*, 82(19), 7871–7878, doi:10.1021/ac100856j, 2010.
- Bzdek, B. R., Zordan, C. A., Luther, G. W. and Johnston, M. V.: Nanoparticle Chemical Composition During New Particle Formation, *Aerosol Sci. Technol.*, 45(8), 1041–1048, doi:10.1080/02786826.2011.580392, 2011.
- Bzdek, B. R., Zordan, C. A., Pennington, M. R., Luther III, G. W. and Johnston, M. V.: Quantitative Assessment of the Sulfuric Acid Contribution to New Particle Growth, *Environ. Sci. Technol.*, 46(8), 4365–4373, doi:10.1021/es204556c, 2012.
- 295 Bzdek, B. R., Horan, A. J., Pennington, M. R., DePalma, J. W., Zhao, J., Jen, C. N., Hanson, D. R., Smith, J. N., McMurry, P. H. and Johnston, M. V.: Quantitative and time-resolved nanoparticle composition measurements during new particle formation, *Faraday Discuss.*, 165, 25–43, doi:10.1039/c3fd00039g, 2013.
- Bzdek, B. R., Lawler, M. J., Horan, A. J., Pennington, M. R., DePalma, J. W., Zhao, J., Smith, J. N. and Johnston, M. V.: Molecular constraints on particle growth during new particle formation, *Geophys. Res. Lett.*, 6045–6054, doi:10.1002/2014GL060160, 2014a.
- 300 Bzdek, B. R., Horan, A. J., Pennington, M. R., Janecek, N. J., Baek, J., Stanier, C. O. and Johnston, M. V.: Silicon is a frequent component of atmospheric nanoparticles, *Environ. Sci. Technol.*, 48(19), 11137–11145, doi:10.1021/es5026933, 2014b.
- 305 Carslaw, K. S., Lee, L. a, Reddington, C. L., Mann, G. W. and Pringle, K. J.: The magnitude and sources of



- uncertainty in global aerosol, *Faraday Discuss.*, 165, 495–512, doi:10.1039/c3fd00043e, 2013.
- Charlson, R. J., Schwartz, S. E., Hales, J. M., Cess, R. D., Coakley, J. A., Hansen, J. E. and Hofmann, D. J.: Climate Forcing by Anthropogenic Aerosols, *Science*, 255, 423–430, 1992.
- Clegg, S. L., Brimblecombe, P. and Wexler, A. S.: Thermodynamic Model of the System H^+ - NH_4^+ - Na^+ - SO_4^{2-} - NO_3^- - Cl^- - H_2O at 298.15 K, *J. Phys. Chem. A*, 5639(3), 2155–2171, doi: 10.1021/jp973042r, 1998.
- 310 De Haan, D. O., Hawkins, L. N., Kononenko, J. A., Turley, J. J. and Jimenez, J. L.: Formation of Nitrogen-Containing Oligomers by Methylglyoxal and Amines in Simulated Evaporating Cloud Droplets, *Environ. Sci. Technol.*, 45(3), 984–991, doi:10.1021/es102933x, 2011.
- Donahue, N. M., Robinson, A. L., Stanier, C. O. and Pandis, S. N.: Coupled Partitioning, Dilution, and Chemical
315 Aging of Semivolatile Organics, *Environ. Sci. Technol.*, 40(8), 2635–2643, doi:10.1021/es052297c, 2006.
- Donahue, N. M., Epstein, S. A., Pandis, S. N. and Robinson, A. L.: A two-dimensional volatility basis set: 1. organic-aerosol mixing thermodynamics, *Atmos. Chem. Phys.*, 11(7), 3303–3318, doi:10.5194/acp-11-3303-2011, 2011a.
- Donahue, N. M., Trump, E. R., Pierce, J. R. and Riipinen, I.: Theoretical constraints on pure vapor-pressure driven
320 condensation of organics to ultrafine particles, *Geophys. Res. Lett.*, 38(16), 3–7, doi:10.1029/2011GL048115, 2011b.
- Donahue, N. M., Kroll, J. H., Pandis, S. N. and Robinson, A. L.: A two-dimensional volatility basis set-Part 2: Diagnostics of organic-aerosol evolution, *Atmos. Chem. Phys.*, 12(2), 615–634, doi:10.5194/acp-12-615-2012, 2012.
- 325 Dusek, U., Frank, G. P., Hildebrandt, L., Curtius, J., Schneider, J., Walter, S., Chand, D., Drewnick, F., Hings, S., Jung, D., Borrmann, S. and Andreae, M. O.: Size Matters More Than Chemistry Aerosol Particles, *Science*, 312(5778), 1375–1378, doi:10.1126/science.1125261, 2006.
- Ehn, M., Kleist, E., Junninen, H., Petäjä, T., Lönn, G., Schobesberger, S., Dal Maso, M., Trimborn, A., Kulmala, M., Worsnop, D. R., Wahner, A., Wildt, J. and Mentel, T. F.: Gas phase formation of extremely oxidized pinene
330 reaction products in chamber and ambient air, *Atmos. Chem. Phys.*, 12(11), 5113–5127, doi:10.5194/acp-12-5113-2012, 2012.
- Ehn, M., Thornton, J. A., Kleist, E., Sipila, M., Junninen, H., Pullinen, I., Springer, M., Rubach, F., Tillmann, R., Lee, B., Lopez-Hilfiker, F., Andres, S., Acir, I. H., Rissanen, M., Jokinen, T., Schobesberger, S., Kangasluoma, J., Kontkanen, J., Nieminen, T., Kurten, T., Nielsen, L. B., Jorgensen, S., Kjaergaard, H. G., Canagaratna, M., Dal
335 Maso, M., Berndt, T., Petaja, T., Wahner, A., Kerminen, V. M., Kulmala, M., Worsnop, D. R., Wildt, J. and Mentel, T. F.: A large source of low-volatility secondary organic aerosol, *Nature*, 506(7489), 476–479, doi:10.1038/Nature13032, 2014.



- 340 Ervens, B. and Volkamer, R.: Glyoxal processing by aerosol multiphase chemistry: Towards a kinetic modeling framework of secondary organic aerosol formation in aqueous particles, *Atmos. Chem. Phys.*, 10(17), 8219–8244, doi:10.5194/acp-10-8219-2010, 2010.
- Galloway, M. M., Powelson, M. H., Sedehi, N., Wood, S. E., Millage, K. D., Kononenko, J. A., Rynaski, A. D. and De Haan, D. O.: Secondary organic aerosol formation during evaporation of droplets containing atmospheric aldehydes, amines, and ammonium sulfate, *Environ. Sci. Technol.*, 48(24), 14417–14425, doi:10.1021/es5044479, 2014.
- 345 Gatzsche, K., Iinuma, Y., Tilgner, A., Mutzel, A., Berndt, T. and Wolke, R.: Modeling studies of SOA formation from α -pinene ozonolysis, *Atmos. Chem. Phys. Discuss.*, doi:10.5194/acp-2017-275, 2017.
- Heaton, K. J., Sleighter, R. L., Hatcher, P. G., Hall IV, W. A. and Johnston, M. V.: Composition domains in monoterpene secondary organic aerosol, *Environ. Sci. Technol.*, 43(20), 7797–7802, doi:10.1021/es901214p, 2009.
- 350 Jimenez, J. L., Canagaratna, M. R., Donahue, N. M., Prevot, A. S. H., Zhang, Q., Kroll, J. H., Decarlo, P. F., Allan, J. D., Coe, H., Ng, N. L., Aiken, A. C., Ulbrich, I. M., Grieshop, A. P., Duplissy, J., Wilson, K. R., Lanz, V. A., Hueglin, C., Sun, Y. L., Tian, J., Laaksonen, A., Raatikainen, T., Rautiainen, J., Vaattovaara, P., Ehn, M., Kulmala, M., Tomlinson, J. M., Cubison, M. J., Dunlea, E. J., Alfarra, M. R., Williams, P. I., Bower, K., Kondo, Y., Schneider, J., Drewnick, F., Borrmann, S., Weimer, S., Demerjian, K., Salcedo, D., Cottrell, L., Takami, A., Miyoshi, T., Shimono, A., Sun, J. Y., Zhang, Y. M., Dzepina, K., Sueper, D., Jayne, J. T., Herndon, S. C., Williams, 355 L. R., Wood, E. C., Middlebrook, A. M., Kolb, C. E., Baltensperger, U. and Worsnop, D. R.: Evolution of Organic Aerosols in the Atmosphere, *Science*, 326, 1525–1529, doi:10.1126/science.1180353, 2009.
- Jokinen, T., Berndt, T., Makkonen, R., Kerminen, V.-M., Junninen, H., Paasonen, P., Stratmann, F., Herrmann, H., Guenther, A. B., Worsnop, D. R., Kulmala, M., Ehn, M. and Sipilä, M.: Production of extremely low volatile organic compounds from biogenic emissions: Measured yields and atmospheric implications, *Proc. Natl. Acad. Sci. U. S. A.*, 112(23), 7123–7128, doi:10.1073/pnas.1423977112, 2015.
- 360 Kalberer, M., Paulsen, D., Sax, M., Steinbacher, M., Dommen, J., Prevot, a S. H., Fisseha, R., Weingartner, E., Frankevich, V., Zenobi, R. and Baltensperger, U.: Identification of polymers as major components of atmospheric organic aerosols., *Science*, 303(5664), 1659–1662, doi:10.1126/science.1092185, 2004.
- Kerminen, V. M., Paramonov, M., Anttila, T., Riipinen, I., Fountoukis, C., Korhonen, H., Asmi, E., Laakso, L., 365 Lihavainen, H., Swietlicki, E., Svenningsson, B., Asmi, A., Pandis, S. N., Kulmala, M. and Petäjä, T.: Cloud condensation nuclei production associated with atmospheric nucleation: A synthesis based on existing literature and new results, *Atmos. Chem. Phys.*, 12(24), 12037–12059, doi:10.5194/acp-12-12037-2012, 2012.
- Kourtchev, I., Giorio, C., Manninen, A., Wilson, E., Mahon, B., Aalto, J., Kajos, M., Venables, D., Ruuskanen, T., Levula, J., Loponen, M., Connors, S., Harris, N., Zhao, D., Kiendler-Scharr, A., Mentel, T., Rudich, Y., Hallquist, 370 M., Doussin, J.-F., Maenhaut, W., Bäck, J., Petäjä, T., Wenger, J., Kulmala, M. and Kalberer, M.: Enhanced Volatile Organic Compounds emissions and organic aerosol mass increase the oligomer content of atmospheric aerosols, *Sci.*



- Rep., 6, 35038, doi:10.1038/srep35038, 2016.
- Kreidenweis, S. M., Koehler, K., DeMott, P., Prenni, a. J., Carrico, C. and Ervens, B.: Water activity and activation diameters from hygroscopicity data - Part I: Theory and application to inorganic salts, *Atmos. Chem. Phys. Discuss.*, 375 5(1), 287–323, doi:10.5194/acpd-5-287-2005, 2005.
- Kroll, J. H. and Seinfeld, J. H.: Chemistry of secondary organic aerosol: Formation and evolution of low-volatility organics in the atmosphere, *Atmos. Environ.*, 42(16), 3593–3624, doi:10.1016/j.atmosenv.2008.01.003, 2008.
- Kuang, C., Riipinen, I., Sihto, S. L., Kulmala, M., McCormick, A. V. and McMurry, P. H.: An improved criterion for new particle formation in diverse atmospheric environments, *Atmos. Chem. Phys.*, 10(17), 8469–8480, 380 doi:10.5194/acp-10-8469-2010, 2010.
- Kuang, C., Chen, M., Zhao, J., Smith, J., McMurry, P. H. and Wang, J.: Size and time-resolved growth rate measurements of 1 to 5 nm freshly formed atmospheric nuclei, *Atmos. Chem. Phys.*, 12(7), 3573–3589, doi:10.5194/acp-12-3573-2012, 2012.
- Kulmala, M., Kontkanen, J., Junninen, H., Lehtipalo, K., Manninen, H. E., Nieminen, T., Petäjä, T., Sipilä, M., 385 Schobesberger, S., Rantala, P., Franchin, A., Jokinen, T., Järvinen, E., Äijälä, M., Kangasluoma, J., Hakala, J., Aalto, P. P., Paasonen, P., Mikkilä, J., Vanhanen, J., Aalto, J., Hakola, H., Makkonen, U., Ruuskanen, T., Mauldin, R. L., Duplissy, J., Vehkamäki, H., Bäck, J., Kortelainen, A., Riipinen, I., Kurtén, T., Johnston, M. V., Smith, J. N., Ehn, M., Mentel, T. F., Lehtinen, K. E. J., Laaksonen, A., Kerminen, V.-M. and Worsnop, D. R.: Direct observations of atmospheric aerosol nucleation, *Science*, 339(6122), 943–6, doi:10.1126/science.1227385, 2013.
- 390 Lee, A. K. Y., Zhao, R., Li, R., Liggio, J., Li, S. M. and Abbatt, J. P. D.: Formation of light absorbing organo-nitrogen species from evaporation of droplets containing glyoxal and ammonium sulfate, *Environ. Sci. Technol.*, 47(22), 12819–12826, doi:10.1021/es402687w, 2013.
- Liu, A. T., Zaveri, R. A. and Seinfeld, J. H.: Analytical solution for transient partitioning and reaction of a condensing vapor species in a droplet, *Atmos. Environ.*, 89, 651–654, doi:10.1016/j.atmosenv.2014.02.065, 2014.
- 395 Lohmann, U. and Feichter, J.: Global indirect aerosol effects: a review, *Atmos. Chem. Phys. Discuss.*, 4(6), 7561–7614, doi:10.5194/acpd-4-7561-2004, 2004.
- Lopez-Hilfiker, F. D., Mohr, C., D'Ambro, E. L., Lutz, A., Riedel, T. P., Gaston, C. J., Iyer, S., Zhang, Z., Gold, A., Surratt, J. D., Lee, B. H., Kurten, T., Hu, W. W., Jimenez, J., Hallquist, M. and Thornton, J. A.: Molecular Composition and Volatility of Organic Aerosol in the Southeastern U.S.: Implications for IEPOX Derived SOA, 400 *Environ. Sci. Technol.*, 50(5), 2200–2209, doi:10.1021/acs.est.5b04769, 2016.
- Mai, H., Shiraiwa, M., Flagan, R. C. and Seinfeld, J. H.: Under What Conditions Can Equilibrium Gas-Particle Partitioning Be Expected to Hold in the Atmosphere?, *Environ. Sci. Technol.*, 49(19), 11485–11491, doi:10.1021/acs.est.5b02587, 2015.



- Pankow, J. F.: An Absorption Model of Gas / Particle Partitioning of Organic Compounds in the Atmosphere, Atmos. Environ., 28(2), 185–188, doi:10.1016/1352-2310(94)90093-0, 1994.
- 405 Pennington, M. R., Bzdek, B. R., Depalma, J. W., Smith, J. N., Kortelainen, A. M., Hildebrandt Ruiz, L., Petäjä, T., Kulmala, M., Worsnop, D. R. and Johnston, M. V.: Identification and quantification of particle growth channels during new particle formation, Atmos. Chem. Phys., 13(20), 10215–10225, doi:10.5194/acp-13-10215-2013, 2013.
- Reinhardt, A., Emmenegger, C., Gerrits, B., Panse, C., Dommen, J., Baltensperger, U., Zenobi, R. and Kalberer, M.:
410 Ultrahigh mass resolution and accurate mass measurements as a tool to characterize oligomers in secondary organic aerosols, Anal. Chem., 79(11), 4074–4082, doi:10.1021/ac062425v, 2007.
- Riccobono, F., Schobesberger, S., Scott, C. E., Dommen, J., Ortega, I. K., Rondo, L., Almeida, J., Amorim, A., Bianchi, F., Breitenlechner, M., David, A., Downard, A., Dunne, E. M., Duplissy, J., Ehrhart, S., Flagan, R. C., Franchin, A., Hansel, A., Junninen, H., Kajos, M., Keskinen, H., Kupc, A., Kurten, A., Kvashin, A. N., Laaksonen, A., Lehtipalo, K., Makhmutov, V., Mathot, S., Nieminen, T., Onnela, A., Petaja, T., Praplan, A. P., Santos, F. D., Schallhart, S., Seinfeld, J. H., Sipila, M., Spracklen, D. V., Stozhkov, Y., Stratmann, F., Tome, A., Tsagkogeorgas, G., Vaattovaara, P., Viisanen, Y., Vrtala, A., Wagner, P. E., Weingartner, E., Wex, H., Wimmer, D., Carslaw, K. S., Curtius, J., Donahue, N. M., Kirkby, J., Kulmala, M., Worsnop, D. R., Baltensperger, U., Kürten, A., Kvashin, A. N., Laaksonen, A., Lehtipalo, K., Makhmutov, V., Mathot, S., Nieminen, T., Onnela, A., Petäjä, T., Praplan, A. P.,
415 Santos, F. D., Schallhart, S., Seinfeld, J. H., Sipilä, M., Spracklen, D. V., Stozhkov, Y., Stratmann, F., Tomé, A., Tsagkogeorgas, G., Vaattovaara, P., Viisanen, Y., Vrtala, A., Wagner, P. E., Weingartner, E., Wex, H., Wimmer, D., Carslaw, K. S., Curtius, J., Donahue, N. M., Kirkby, J., Kulmala, M., Worsnop, D. R. and Baltensperger, U.:
420 Oxidation Products of Biogenic Emissions Contribute to Nucleation of Atmospheric Particles, Science, 344(6185), 717–721, doi:10.1126/science.1243527, 2014.
- 425 Riipinen, I., Yli-Juuti, T., Pierce, J. R., Petäjä, T., Worsnop, D. R., Kulmala, M. and Donahue, N. M.: The contribution of organics to atmospheric nanoparticle growth, Nat. Geosci., 5(7), 453–458, doi:10.1038/ngeo1499, 2012.
- Riva, M., Budisulistiorini, S. H., Chen, Y., Zhang, Z., D'Ambro, E. L., Zhang, X., Gold, A., Turpin, B. J., Thornton, J. A., Canagaratna, M. R. and Surratt, J. D.: Chemical Characterization of Secondary Organic Aerosol from
430 Oxidation of Isoprene Hydroxyhydroperoxides, Environ. Sci. Technol., 50(18), 9889–9899, doi:10.1021/acs.est.6b02511, 2016.
- Saul, T. D., Tolocka, M. P. and Johnston, M. V.: Reactive uptake of nitric acid onto sodium chloride aerosols across a wide range of relative humidities, J. Phys. Chem. A, 110(24), 7614–7620, doi:10.1021/jp060639a, 2006.
- Shiraiwa, M., Pfrang, C., Koop, T. and Pöschl, U.: Kinetic multi-layer model of gas-particle interactions in aerosols
435 and clouds (KM-GAP): Linking condensation, evaporation and chemical reactions of organics, oxidants and water, Atmos. Chem. Phys., 12(5), 2777–2794, doi:10.5194/acp-12-2777-2012, 2012.
- Shiraiwa, M., Zuend, A., Bertram, A. K. and Seinfeld, J. H.: Gas-particle partitioning of atmospheric aerosols:



- interplay of physical state, non-ideal mixing and morphology., *Phys. Chem. Chem. Phys.*, 15(27), 11441–53, doi:10.1039/c3cp51595h, 2013.
- 440 Shiraiwa, M., Berkemeier, T., Schilling-Fahnestock, K. A., Seinfeld, J. H. and Pöschl, U.: Molecular corridors and kinetic regimes in the multiphase chemical evolution of secondary organic aerosol, *Atmos. Chem. Phys.*, 14(16), 8323–8341, doi:10.5194/acp-14-8323-2014, 2014.
- Smith, G. D., Woods III, E., Baer, T. and Miller, R. E.: Aerosol Uptake Described by Numerically Solving the Diffusion-Reaction Equations in the Particle, *J. Phys. Chem. A*, 107, 9582–9587, doi:10.1021/jp021843a, 2003.
- 445 Song, M., Liu, P. F., Hanna, S. J., Li, Y. J., Martin, S. T. and Bertram, A. K.: Relative humidity-dependent viscosities of isoprene-derived secondary organic material and atmospheric implications for isoprene-dominant forests, *Atmos. Chem. Phys.*, 15(9), 5145–5159, doi:10.5194/acp-15-5145-2015, 2015.
- Stangl, C. M. and Johnston, M. V.: Aqueous Reaction of Dicarboxyls with Ammonia as a Potential Source of Organic Nitrogen in Airborne Nanoparticles, *J. Phys. Chem. A*, doi:10.1021/acs.jpca.7b02464, 2017.
- 450 Surratt, J. D., Lewandowski, M., Offenberg, J. H., Kleindienst, T. E., Edney, E. O., Seinfeld, J. H. and Surratt, J. D.: Effect of Acidity on Secondary Organic Aerosol Formation from Isoprene Effect of Acidity on Secondary Organic Aerosol Formation from Isoprene, *Environ. Sci. Technol.*, 41(15), 5363–5369, doi:10.1021/es0704176, 2007.
- Tolocka, M. P., Jang, M., Ginter, J. M., Cox, J., Kamens, R. M., Johnston, M. V. and Tolocka, M. P.: Formation of Oligomers in Secondary Organic Aerosol, , 38(5), 1428–1434, doi:10.1021/es035030r, 2004a.
- 455 Tolocka, M. P., Saul, T. D. and Johnston, M. V.: Reactive uptake of nitric acid into aqueous sodium chloride particles using real-time single-particle mass spectrometry, *J. Phys. Chem. A*, 108, 2659–2665, doi:10.1021/jp036612y, 2004b.
- Tröstl, J., Chuang, W. K., Gordon, H., Heinritzi, M., Yan, C., Molteni, U., Ahlm, L., Frege, C., Bianchi, F., Wagner, R., Simon, M., Lehtipalo, K., Williamson, C., Craven, J. S., Duplissy, J., Adamov, A., Almeida, J., Bernhammer, A.-K., Breitenlechner, M., Brilke, S., Dias, A., Ehrhart, S., Flagan, R. C., Franchin, A., Fuchs, C., Guida, R., Gysel, M., Hansel, A., Hoyle, C. R., Jokinen, T., Junninen, H., Kangasluoma, J., Keskinen, H., Kim, J., Krapf, M., Kürten, A., Laaksonen, A., Lawler, M., Leiminger, M., Mathot, S., Möhler, O., Nieminen, T., Onnela, A., Petäjä, T., Piel, F. M., Miettinen, P., Rissanen, M. P., Rondo, L., Sarnela, N., Schobesberger, S., Sengupta, K., Sipilä, M., Smith, J. N., Steiner, G., Tomè, A., Virtanen, A., Wagner, A. C., Weingartner, E., Wimmer, D., Winkler, P. M., Ye, P., Carslaw, K. S., Curtius, J., Dommen, J., Kirkby, J., Kulmala, M., Riipinen, I., Worsnop, D. R., Donahue, N. M. and Baltensperger, U.: The role of low-volatility organic compounds in initial particle growth in the atmosphere, *Nature*, 533(7604), 527–531, doi:10.1038/nature18271, 2016.
- Trump, E. R. and Donahue, N. M.: Oligomer formation within secondary organic aerosols: equilibrium and dynamic considerations, *Atmos. Chem. Phys.*, 14, 3691–3701, doi:10.5194/acp-14-3691-2014, 2014.
- 470 Tu, P. and Johnston, M. V.: Particle Size Dependence of Biogenic Secondary Organic Aerosol Molecular



- Composition, Atmos. Chem. Phys. Discuss., DOI:10.5194/acp-2017-53, doi:10.5194/acp-2017-53, 2017.
- Tu, P., Hall, W. A. and Johnston, M. V.: Characterization of Highly Oxidized Molecules in Fresh and Aged Biogenic Secondary Organic Aerosol, *Anal. Chem.*, 88(8), 4495–4501, doi:10.1021/acs.analchem.6b00378, 2016.
- 475 Vestenius, M., Hellén, H., Levula, J., Kuronen, P., Helminen, K. J., Nieminen, T., Kulmala, M. and Hakola, H.: Acidic reaction products of monoterpenes and sesquiterpenes in atmospheric fine particles in a boreal forest, *Atmos. Chem. Phys.*, 14(15), 7883–7893, doi:10.5194/acp-14-7883-2014, 2014.
- Weber, R. J., Marti, J. J. and McMurry, P. H.: Measured Atmospheric New Particle Formation Rates: Implications for Nucleation Mechanisms, *Chem. Eng. Comm.*, 151, 53–64, 1996.
- 480 Wexler, A. S. and Clegg, S. L.: Atmospheric aerosol models for systems including the ions H⁺, NH₄⁺, Na⁺, SO₄²⁻, NO₃⁻, Cl⁻, Br⁻, and H₂O, *J. Geophys. Res.*, 107, 1–14, doi:10.1029/2001JD000451, 2002.
- Winkler, P. M., Ortega, J., Karl, T., Cappellin, L., Friedli, H. R., Barsanti, K., McMurry, P. H. and Smith, J. N.: Identification of the biogenic compounds responsible for size-dependent nanoparticle growth, *Geophys. Res. Lett.*, 39(20), 1–6, doi:10.1029/2012GL053253, 2012.
- 485 Wong, J. P. S., Lee, A. K. Y. and Abbatt, J. P. D.: Impacts of Sulfate Seed Acidity and Water Content on Isoprene Secondary Organic Aerosol Formation, *Environ. Sci. Technol.*, 49(22), 13215–13221, doi:10.1021/acs.est.5b02686, 2015.
- Wu, Y. and Johnston, M. V.: Aerosol Formation from OH Oxidation of the Volatile Cyclic Methyl Siloxane (cVMS) Decamethylcyclopentasiloxane, *Environ. Sci. Technol.*, 51, 4445–4451, doi:10.1021/acs.est.7b00655, 2017.
- 490 Xu, L., Guo, H., Boyd, C. M., Bougiatioti, A., Cerully, K. M., Hite, J. R., Isaacman-vanwertz, G., Kreisberg, N. M., Olson, K., Koss, A., Goldstein, A. H., Susanne, V., Gouw, J. De, Baumann, K., Lee, S., Nenes, A., Weber, R. J. and Ng, N. L.: Effects of anthropogenic emissions on aerosol formation from isoprene and monoterpenes in the southeastern United States, *Proc. Natl. Acad. Sci.*, 112(32), 37–42, doi:10.1073/pnas.1512277112, 2015.
- Yli-Juuti, T., Barsanti, K., Hildebrandt Ruiz, L., Kieloaho, A. J., Makkonen, U., Petäjä, T., Ruuskanen, T., Kulmala, M. and Riipinen, I.: Model for acid-base chemistry in nanoparticle growth (MABNAG), *Atmos. Chem. Phys.*, 13(24), 12507–12524, doi:10.5194/acp-13-12507-2013, 2013.
- 495 Zaveri, R. A., Easter, R. C., Shilling, J. E. and Seinfeld, J. H.: Modeling kinetic partitioning of secondary organic aerosol and size distribution dynamics: Representing effects of volatility, phase state, and particle-phase reaction, *Atmos. Chem. Phys.*, 14(10), 5153–5181, doi:10.5194/acp-14-5153-2014, 2014.
- Zhang, R., Khalizov, A., Wang, L., Hu, M. and Xu, W.: Nucleation and growth of nanoparticles in the atmosphere, 500 *Chem. Rev.*, 112, 1957–2011, doi:10.1021/cr2001756, 2012.
- Zhao, J., Ortega, J., Chen, M., McMurry, P. H. and Smith, J. N.: Dependence of particle nucleation and growth on high-molecular-weight gas-phase products during ozonolysis of α -pinene, *Atmos. Chem. Phys.*, 13(15), 7631–7644,



doi:10.5194/acp-13-7631-2013, 2013.

505



Tables and Figures

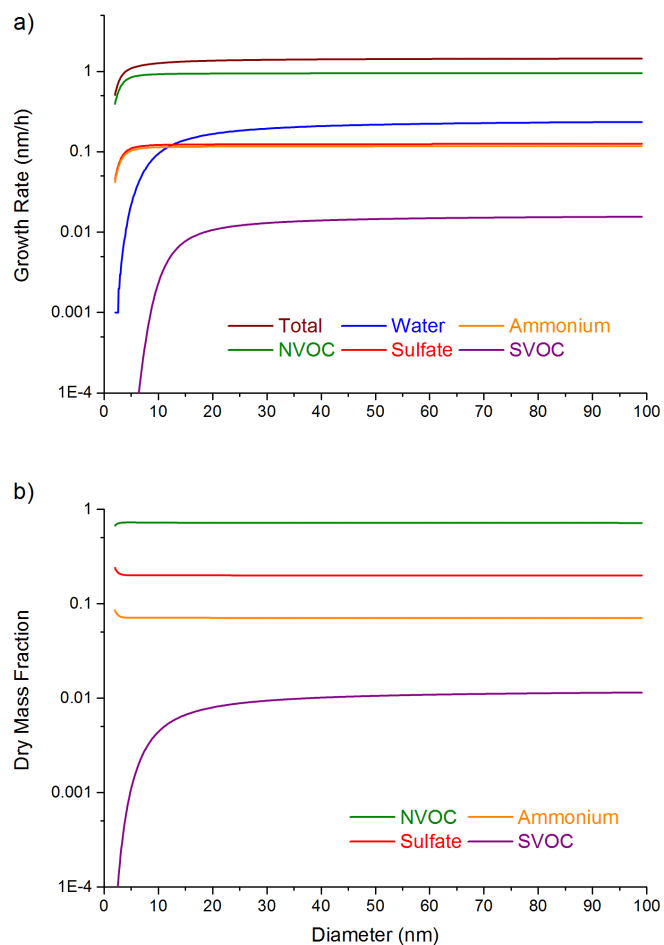
Table 1: Mixing ratios and relevant physical properties of chemical species included in particle growth calculations.

(T = 282 °C, RH = 50%)

	Mixing Ratio, $C_{i,g}$		Saturation Concentration	Molar Mass	Density
	ng m^{-3}	ppt	$\log C^*$, ($\mu\text{g m}^{-3}$)	g mol^{-1}	g cm^{-3}
Sulfuric Acid	0.5	0.12	-	98	1.8
Ammonia	1	1.25	-	17	0.7
SVOC	3-11	0.4-1.4	10^0	200	1.2
NVOC	3	0.4	10^{-4}	200	1.2
DIMER	-	-	-	400	1.2



510

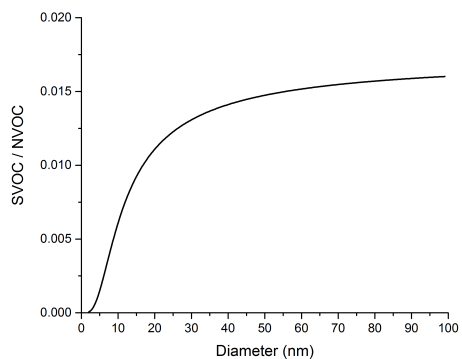


511

512 **Figure 1:** Particle diameter dependence of a) growth rates and b) dry mass fractions of chemical species under the
513 conditions where the gas phase mixing ratios are constant and growth occurs by partitioning alone.

514

515

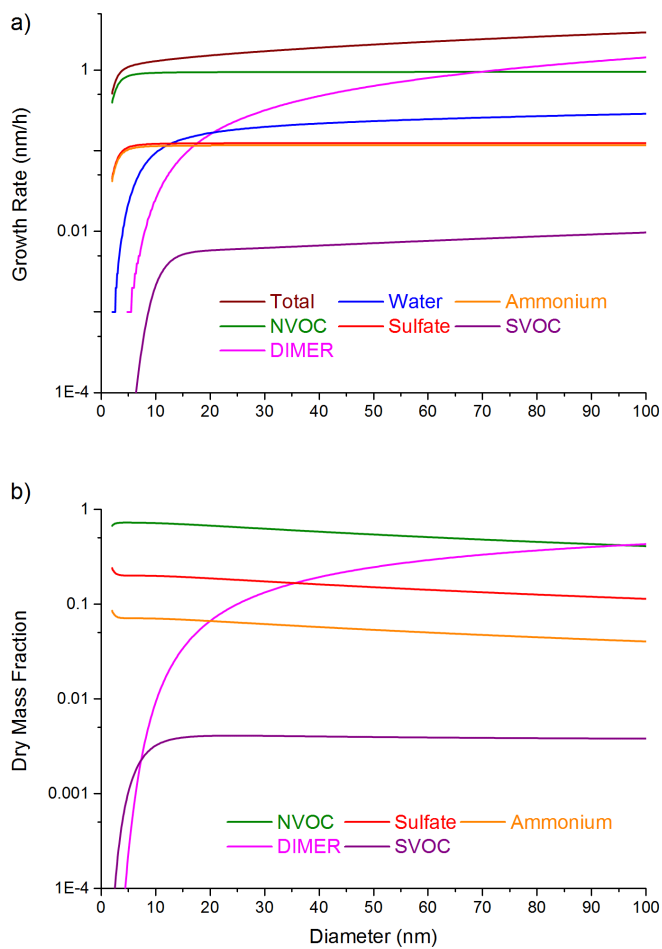


516

517 **Figure 2:** Mass fraction ratio of SVOC / NVOC vs. particle diameter under conditions where growth occurs by
518 partitioning alone.

519

520



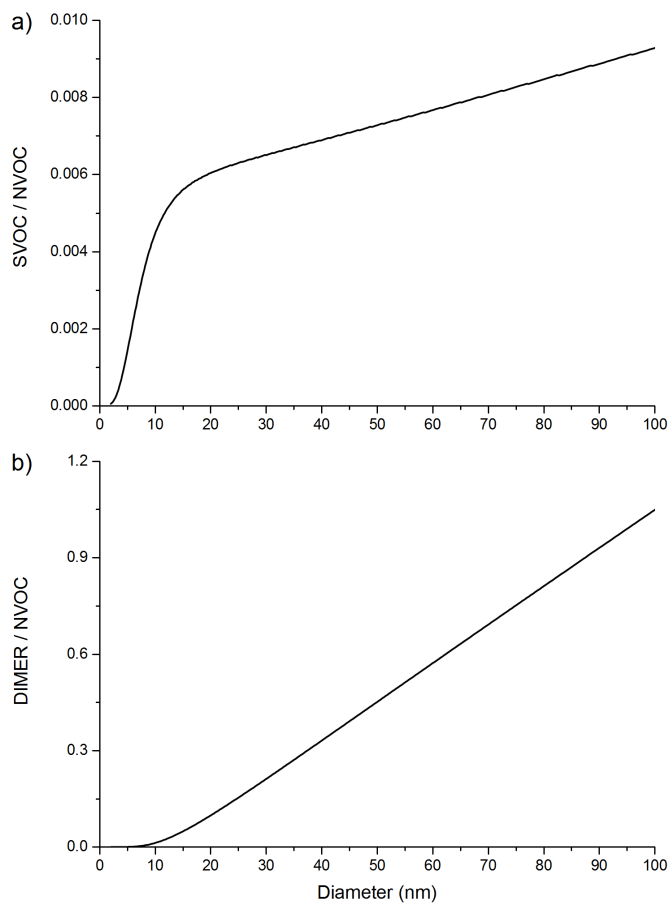
521

522 **Figure 3:** Particle diameter dependence of a) growth rates and b) dry mass fractions of chemical species under the

523 conditions where both partitioning and particle phase chemistry are included.

524

525

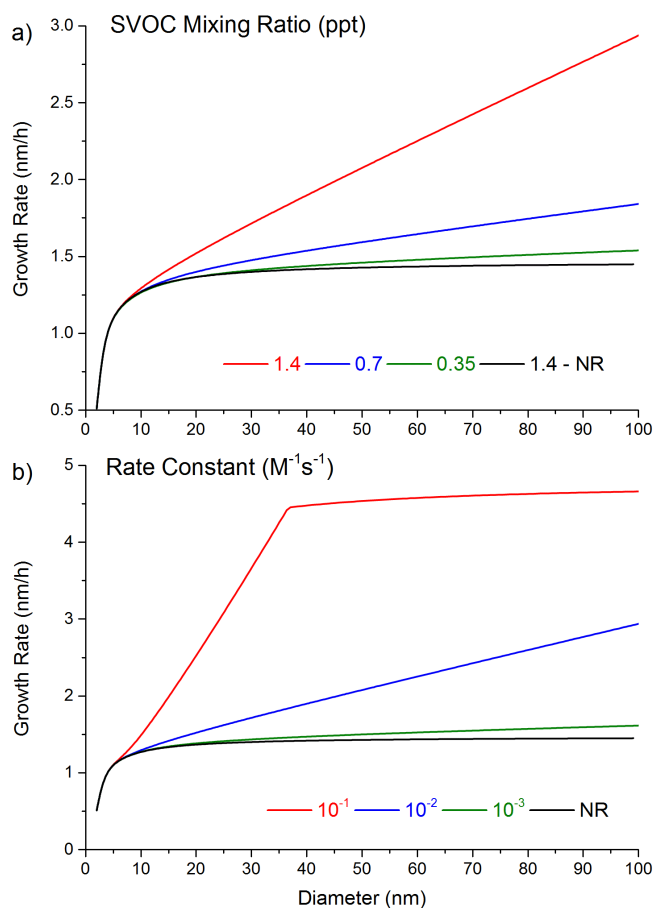


526

527 **Figure 4:** Mass ratio of a) SVOC to NVOC vs. particle diameter and b) Dimer to NVOC, under conditions where
528 both partitioning and particle phase chemistry are included.

529

530



531

532 **Figure 5:** Growth rate vs. particle diameter for a) varying SVOC mixing ratio, and b) varying DIMER formation
533 rate constant in the particle phase under conditions where both partitioning and particle phase chemistry are
534 included. In these plots, the black line indicates the particle diameter dependence in Figure 1a.

535

536